Atom-laser coherence length and atomic standing waves

I. Carusotto,[1,4,*] M. Artoni,[2] and G. C. La Rocca[3,4]
[1]*Scuola Normale Superiore, Piazza dei Cavalieri 7, 56126 Pisa, Italy*
[2]*INFM, European Laboratory for Non-Linear Spectroscopy, Largo E. Fermi 2, 50125 Florence, Italy*
[3]*Dipartimento di Fisica, Università di Salerno, 84081 Baronissi (SA), Italy*
[4]*INFM, Scuola Normale Superiore, Piazza dei Cavalieri 7, 56126 Pisa, Italy*
(Received 14 April 2000; revised manuscript received 5 September 2000; published 14 November 2000)

We consider the dynamical Bragg reflection of an atomic matter wave from a finite optical lattice; the resulting energy dependence of the transmittivity allows us to filter out the velocities of the incident atoms. In particular, we show how the coherence length of the incident beam can be inferred from the sharpness of the transmittivity as a function of the lattice intensity. For incident frequencies well inside the reflecting window, the interference of incident and reflected matter waves gives rise to an oscillatory density profile in front of the lattice which can be observed by means of light diffraction. The angular width of the diffracted peaks also provides information on the coherence length of the incident atomic beam.

PACS number(s): 03.75.Be, 03.75.Fi, 42.25.Fx

The recent advances in the preparation of Bose-Einstein-condensed atomic samples [1] and coherent atomic beams [2] has attracted the attention of both theorists [3] and experimentalists [4] on the characterization of the coherence properties of such ultra-low-temperature interacting Bose-Einstein systems. The present paper proposes two possible methods for the determination of the coherence length of a weak propagating atomic beam; unlike other schemes, our proposals do not involve the properties of the parent condensate.

The first method (Sec. I) adapts ideas from the dynamical theory of x-ray scattering [5,6] and photonic band-gap crystals [7] to the coherent reflection of atoms from optical lattices [8,9]. The frequency dependence of the transmittivity enables one to filter the different frequency components in the incident beam so as to determine the spectral distribution. The second method (Sec. II) is based on optical diffraction [10] on the atomic standing wave which is present in front of a nearly perfect atomic mirror. Light is diffracted by the phase grating provided by the atomic density modulation and the coherence length is inferred from the angular line shape of the first-order diffracted peaks.

I. VELOCITY FILTERING

Consider a weak and collimated atomic beam that propagates along the z axis of an optical lattice formed by a pair of nearly counterpropagating laser beams of frequency ω_L and wave vector $k_L=\omega_L/c$. Let $\Omega_L(z)=|\vec{d}\cdot\vec{E}(z)|/\hbar$ be the (slowly varying) single beam Rabi frequency and ω_0 the frequency of the atomic transition. The optical potential experienced by the atoms in a far-detuned optical lattice is conservative and equal to $V^{opt}(z)=\hbar\Omega_0(z)\cos^2 k_L z$, with $\Omega_0(z)=\Omega_L(z)^2/(\omega_L-\omega_0)$. Depending on the positive or negative sign of the laser field detuning $\delta=\omega_L-\omega_0$, this potential is, respectively, repulsive or attractive [11].

The atomic dispersion in the periodic potential of an infinite lattice is characterized by allowed bands and forbidden gaps [12,13]. When the depth Ω_0 of the optical potential is small as compared to the Bragg frequency of the lattice $\omega_{Br}=\hbar k_L^2/2m$ (m being the free-space atomic mass), the band structure is accurately described using the nearly-free-*atom* approximation. For a red detuned ($\delta<0$) lattice, such an approximation leads to a conduction-band lower-edge frequency $\omega_c=\omega_{Br}-\Omega_0/4$ and to a valence-band upper-edge frequency $\omega_v=\omega_{Br}-3\Omega_0/4$.

Consider now the finite optical lattice formed by a pair of nearly counterpropagating laser beams shown in Fig. 1. The atom laser beam impinges on the lattice along a direction parallel to the axis. If the lattice transverse dimensions are wide enough, the transverse dynamics of the matter wave can be neglected and all calculations can be performed considering only the motion along the longitudinal z direction. This approach is clearly exact when the transverse atomic motion

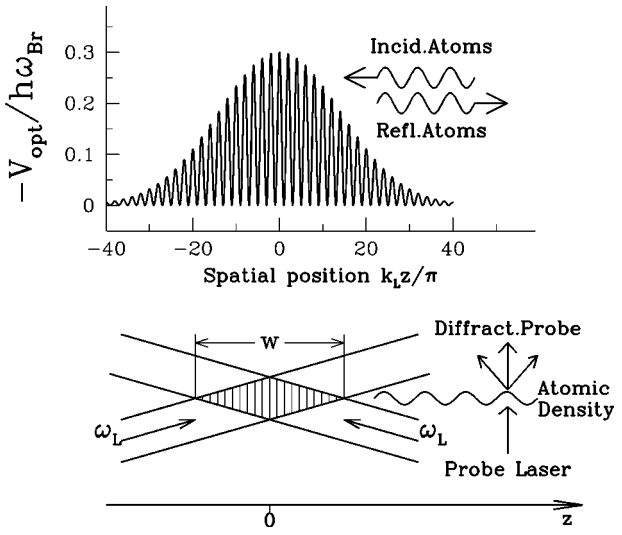

FIG. 1. Lower panel: proposed experimental scheme. Upper panel: qualitative plot of the optical potential experienced by the atoms.

*Email address: Iacopo.Carusotto@sns.it

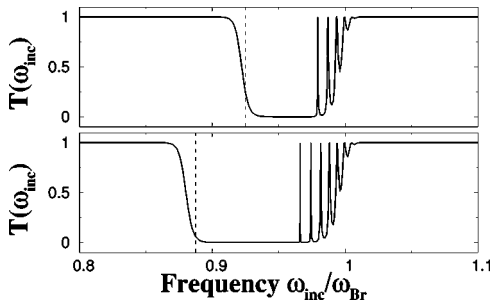

FIG. 2. Transmission spectra for $w=120/k_L$ and lattice intensity $\Omega_0=0.1\omega_{Br}$ (upper) and $\Omega_0=0.15\omega_{Br}$ (lower). Dashed vertical lines correspond to the reflecting window lower edge $\omega_v^{(min)}$.

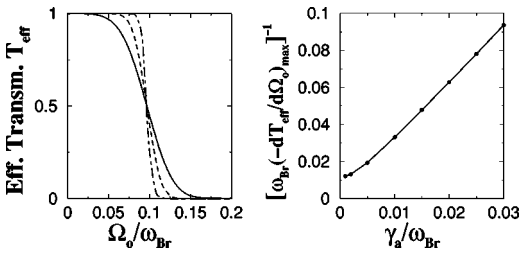

FIG. 3. Left panel: effective transmittivity vs lattice intensity Ω_0 for an incident atomic beam Gaussian linewidth $\gamma_a/\omega_{Br}=0.02$ (solid line), $\gamma_a/\omega_{Br}=0.01$ (dashed line), and $\gamma_a/\omega_{Br}=0.001$ (dot-dashed line). Right panel: Maximum slope $dT_{eff}/d\Omega_0$ vs Gaussian linewidth γ_a. The lattice length is $w=60/k_L$ while the central frequency $\omega_a/\omega_{Br}=0.925$ is such that $\omega_v^{(min)}=\omega_a$ for $\Omega_0/\omega_{Br}=0.1$

is confined by a single-mode atomic waveguide [14]; this enables one to avoid effects due to gravity as well, just by making atoms propagate horizontally. The longitudinal envelope of the lattice is determined by the profile of the laser beam waist and can be described by a Gaussian $\Omega_0(z)=\Omega_0 e^{-z^2/2w^2}$ with $k_L w \gg 1$.

In Fig. 2 we have reported the result of the numerical integration of the linear Schrödinger equation describing the atomic motion in the optical potential of the lattice [15]. The atomic transmittivity $T(\omega_{inc})$, defined as the ratio of the transmitted and the incident intensities, is plotted as a function of the frequency ω_{inc} of the incident atoms for different values of the lattice intensity Ω_0. The nonlinear terms which would arise from a mean-field treatment of atom-atom interactions have been neglected under a weak incident beam assumption. Complete transmission is found at incident frequencies ω_{inc} above the Bragg frequency ω_{Br} or below the minimum value $\omega_v^{(min)}$ of the valence-band upper-edge frequency, while there is nearly complete reflection in the $\omega_v^{(min)}<\omega_{inc}<\omega_{Br}$ frequency window. In one case there are in fact propagating states available at any spatial position z in either the conduction or valence band and therefore the atoms are free to propagate through the lattice. In the other case, instead, atoms enter the lattice in the valence band and are free to propagate only up to the point at which $\omega_v(z)=\omega_{inc}$; afterwards, propagation is no longer possible and atoms are coherently reflected back [8,9,15]. The very narrow spectral peaks which are present at frequencies just below the upper edge ω_{Br} of the reflecting window are due to resonant tunneling processes on conduction-band localized states. The weakness of such Fabry-Perot (FP) peaks is a consequence of the fact that these modes are coupled to the externally propagating modes only by nonadiabatic interband jumps [15]. In any case, the conservative nature of the optical potential V^{opt} guarantees that the sum of the transmitted and the reflected intensities equals the incident one.

The nontrivial dependence of the transmittivity $T(\omega_{inc})$ on the incident frequency ω_{inc} suggests the use of optical lattices as frequency filters for matter waves. By varying the parameters of the lattice, specifically the intensity Ω_0, and by monitoring the density of the transmitted beam during each scan, it is possible to get information on the spectral distribution $S_{inc}(\omega)$ of the incident beam. Since the incident beam is assumed to be stationary, the different frequency components are not correlated $\langle a_{inc}^*(\omega)a_{inc}(\omega')\rangle = S_{inc}(\omega)\delta(\omega-\omega')$ and the time correlation function $\langle a_{inc}^*(t)a_{inc}(0)\rangle = g^{(1)}(t)\langle a_{inc}^*(0)a_{inc}(0)\rangle$ is the Fourier transform of the spectral distribution $S_{inc}(\omega)$. Although the behavior for other line shapes can be shown to be qualitatively very similar, we shall consider in the present section only the case of a Gaussian line shape centered at ω_a with a linewidth equal to γ_a; the characteristic decay time of the correlation function is thus equal to $\tau_a=\gamma_a^{-1}$ [17]. Unlike the previous studies of dynamical diffraction of atoms from optical lattices in which thermal atomic sources were used [8], the present work is mainly focused on coherent atom laser beams, for which γ_a/ω_a is much smaller than 1. Owing to the assumption of negligible atom-atom interactions, the transmitted spectral distribution can be expressed in terms of the incident one, i.e., $S_{tr}(\omega)=T(\omega)S_{inc}(\omega)$. In particular, since the total densities in the incident and transmitted beams are related to the spectral densities $\rho_{inc,tr}=\int S_{inc,tr}(\omega)d\omega$, the effective transmittivity $T_{eff}=\rho_{tr}/\rho_{inc}$ can be easily evaluated.

In the case of a red-detuned optical lattice, the upper edge of the reflecting window is fixed at ω_{Br}, while the position of the lower edge is a linear function of the lattice intensity Ω_0. If ω_a is located below the Bragg frequency ω_{Br}, the atomic beam is completely transmitted for small values of Ω_0, while it is reflected for large values of Ω_0. The width of the crossover region provides information on the atomic linewidth γ_a: in Fig. 3(a) we have plotted the effective transmittivity T_{eff} as a function of the lattice intensity Ω_0, while in Fig. 3(b) we have plotted the maximum of the slope $dT_{eff}/d\Omega_0$, i.e., its value at Ω_0 such as $\omega_v^{(min)}(\Omega_0)=\omega_a$ as a function of γ_a. This latter dependence can be used in an experiment for the determination of the linewidth γ_a of a source. The minimum value of γ_a that can be handled by this method is fixed by the slope of $T(\omega)$ at the edge of the reflecting window; sharper spectra can be, however, obtained using longer lattices.

In the language of x-ray diffraction [5,6], the opening of a finite frequency window with nearly total reflection can be interpreted as a signature of a *dynamical* diffraction process rather than a simple *kinematical* diffraction one. The crossover from a transmitting to a reflecting regime can be reformulated in spatial terms as the crossover from a $l_c<l_e$ to a

$l_c > l_e$ regime, l_e being the extinction length of the optical lattice [7] and $l_c = v_g \tau_a$ the coherence length of the source [17] (v_g is the group velocity of the incident atoms $v_g \approx \hbar k_L / m$). In the latter case constructive interference enhances the reflection amplitude, while in the former case interference is washed out by the limited coherence length of the source. Analogously, dynamical x-ray diffraction effects are washed out if the size of the scattering monocrystals is smaller than the extinction length [5,6].

If the linewidth of the source is smaller than the frequency separation of adjacent FP modes [15], the corresponding resonance peaks can also be used for a spectral analysis of the incident beam. Monitoring the variation of T_{eff} during a scan of the FP mode frequency across the atomic source line shape can provide detailed information on the atomic spectral distribution. Unfortunately, the use of the conduction-band localized states previously described is difficult because of their sensitivity to lattice asymmetries which may hide them from the actual transmission spectra. More complicated configurations could, however, be used to enhance the strength of the peaks, e.g., bichromatic optical lattices as described in [15].

II. ATOMIC STANDING WAVES

In the present section we consider a specific model for the coherence properties of an atom laser which allows for a completely analytical analysis; however, no qualitative differences in the physical behavior are expected to arise from a different form of the statistical properties. The atomic matter field of the atom laser is described as a plane wave of weak intensity $|a_0|^2$, wave vector k_a, frequency $\omega = \hbar k_a^2/2m$, and group velocity $v_g = \hbar k_a / m$ with a slowly diffusing phase ϕ

$$a_{inc}(z,t) = a_0 e^{i(k_a z - \omega_a t)} e^{i\phi(z - v_g t)}. \tag{1}$$

Provided phase coherence is maintained over a characteristic length l_c much longer than the atom laser wavelength, the parabolic atomic dispersion can be approximated as a linear one in a neighborhood of ω_a so that Eq. (1) is a good solution of the atomic Schrödinger equation within a sort of slowly varying envelope approximation ([16], p. 216, and following). Phase diffusion can be modeled in a standard way [17] by the following stochastic differential equation $d\phi(z) = \sqrt{\eta} dB$ with $\langle dB \rangle = 0$, $\langle dB^2 \rangle = dz$; its strength is fixed by the η parameter. By means of simple stochastic techniques [18], the correlation function of such a beam can be shown to be equal to $\langle a^*_{inc}(t) a_{inc}(t') \rangle = |a_0|^2 \exp(-\eta v_g |t - t'|/2)$, so that the spectral distribution $S_{inc}(\omega)$ now has a Lorentzian shape with a linewidth $\gamma_a = \eta v_g / 2$.

When such a beam normally incides on a nearly perfectly reflecting atomic mirror whose reflection bandwidth is much larger than γ_a, we expect that an atomic standing wave is created in front of the mirror. If the beam propagates along the negative-z direction and the mirror is located at $z = 0$, the atomic field amplitude in front of the mirror can be written as a sum of the incident and reflected field amplitudes $a(z,t) = a_{inc}(-z - v_g t) + a_{inc}(z - v_g t + 2 l_{pen}) e^{i\phi_r}$; the penetration depth l_{pen} is defined in terms of the frequency derivative of the reflection phase ϕ_r of the mirror as

$$l_{pen} = \frac{v_g}{2} \frac{\partial \phi_r}{\partial \omega_{inc}}$$

(Ref. [7]). In front of the atomic mirror, interference between the incident and the reflected matter waves creates a standing-wave profile in the atomic density

$$\rho(z,t) = 2|a_0|^2 \{1 + \mathrm{Re}[e^{2ik_L z} e^{i\theta(z,t)}]\} \tag{2}$$

whose contrast is unity at all positions, but whose phase $\theta(z,t) = \phi(z - v_g t + 2 l_{pen}) + \phi_r - \phi(-z - v_g t)$, i.e., the position of its nodes, slowly fluctuates in both space and time [19]. From a simple calculation [18], the correlation function of the phase at a given time t results equal to $\langle e^{i\theta(z,t)} e^{-i\theta(z',t)} \rangle = e^{-\eta |z - z'|}$ which means that the characteristic length over which the phase of the standing-wave decoheres is equal to half the atom laser coherence length l_c. As we can see in Fig. 4, sufficiently close to the mirror [i.e., for $z < (l_c - l_{pen})$], the position of the nodes of the standing wave is locked by the reflection phase of the mirror; farther away it is instead freely fluctuating and the oscillations in the density profile are washed out when averaged over time: at each location z for which $z \gg (l_c - l_{pen})$, the standing-wave position fluctuates in fact within a characteristic time scale set by l_c / v_g.

Since the spatial period of such density fringes is fixed by the wavelength of the matter wave, typically as small as an optical wavelength, the experimental observation of the fringes would require a spatial resolution well beyond the possibilities of any direct imaging system. This difficulty can

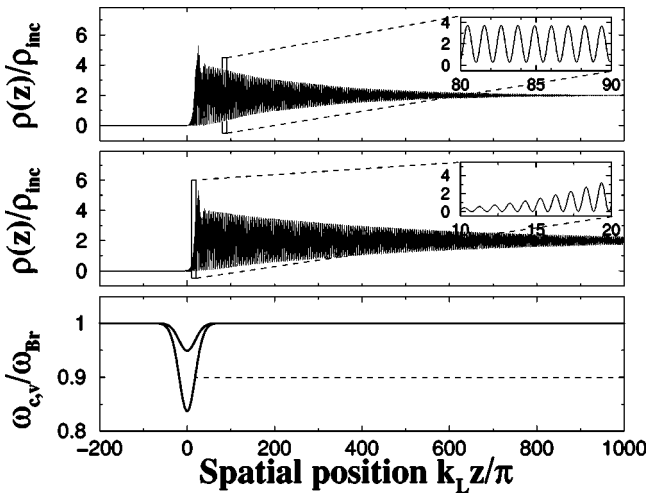

FIG. 4. Mean value of the atomic density profile for an incident atomic beam Lorentzian linewidth $\gamma_a / \omega_{Br} = 6 \times 10^{-4}$ (upper) and $\gamma_a / \omega_{Br} = 3 \times 10^{-4}$ (middle). The broader the linewidth, the faster the phase decoherence of the standing wave leading to the effective decay of the oscillations in the *mean* atomic density. Spatial profile of the local band edges (lower panel). The central frequency $\omega_a / \omega_{Br} = 0.9$ of the Lorentzian source line shape (horizontal dashed line) lies well inside the reflecting window of the DBR atomic mirror with $\Omega_0 / \omega_{Br} = 0.2$.

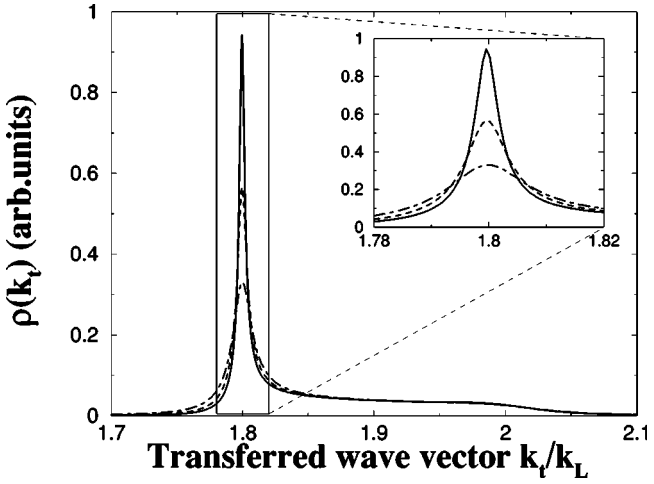

FIG. 5. Angular diffraction pattern for different values of the atom laser linewidth: $\gamma_a/\omega_{Br}=3\times10^{-4}$ (solid line), $\gamma_a/\omega_{Br}=6\times10^{-4}$ (dashed line), and $\gamma_a/\omega_{Br}=1.2\times10^{-3}$ (dot-dashed line). Inset: enlargement of the Bragg peak at $k_t\simeq2\times0.9k_L$ which corresponds to the standing-wave pattern in front of the DBR atomic mirror.

be overcome looking at the diffraction of the light of a probe laser beam on the phase grating provided by the atomic density $\rho(z)$ profile: the spatially modulated refraction index is determined by the refractive properties of the atoms and is proportional to the atomic density $\rho(z)$ [20]. If the probe beam is taken to be far off resonance from any atomic transition, the optical density of the matter wave turns out to be very small and the diffraction process can be treated in the first Born approximation, which takes into account only single scattering processes.

If we denote with $E_p(z)$ the transverse amplitude of an incident probe beam of carrier wave vector k_p and waist σ_p and we assume it to be much broader than the coherence length of the atom laser ($\sigma_p\gg l_c$) and not to spatially overlap with the atomic mirror, the emerging beam profile can be written to lowest order in $\beta\rho$ as $E_e(z,t)=[1+i\beta\rho(z,t)]E_p(z)$ where β is a numerical coefficient proportional to the atomic polarizability and the atom laser beam waist. The scattered amplitude E_s at an angle α is therefore given by

$$E_s(\alpha,t)=\int\frac{dz}{2\pi}e^{-ik_tz}E_e(z,t)$$

$$=\int\frac{dz}{2\pi}e^{-ik_tz}[1+i\beta\rho(z,t)]E_p(z), \qquad (3)$$

where the transferred wave vector k_t is defined as $k_t=k_p\sin\alpha$. If we limit our attention to the scattering at an angle close to the Bragg condition $k_t=2k_a$, all other contributions can be neglected being integrals of fast oscillating functions and Eq. (3) takes the simpler form

$$E_s(\alpha,t)\simeq\beta|a_0|^2\int\frac{dz}{2\pi}e^{(2k_a-k_t)z}e^{i\theta(z,t)}E_p(z). \qquad (4)$$

Experimentally, a detector placed at an angle α would record a signal proportional to the mean intensity of the scattered light $I(\alpha)=\langle|E_s(\alpha)|^2\rangle$.

As $\sigma_p\gg l_c$, the broadening due to the finite coherence of the standing-wave profile here described is much larger than the broadening due to the finite laser waist σ_p, so that the line shape of the scattered light results proportional to

$$I(\alpha)\propto\frac{\eta}{(k_p\sin\alpha-2k_a)^2+\eta^2}. \qquad (5)$$

This means that the coherence length of the atom laser can be retrieved from the angular linewidth of the Bragg peak. Such an effect is physically analogous to the broadening of the diffraction peaks from crystals which occurs in the presence of disorder; our specific phase-diffusion model corresponds to the case of an uneven separation of lattice planes [6].

If the probe beam has a non-negligible overlap with the optical potential of the mirror, the atomic density profile experienced by the probe is not simply the one given by Eq. (2) but presents additional features due to the complicate shape of the atomic wave function inside the distributed Bragg reflector (DBR) mirror. The corresponding line shape for the scattered light is plotted in Fig. 5: in addition to the Lorentzian peak at $k_t\simeq2k_a$ corresponding to the diffraction on the standing-wave pattern in front of the DBR atomic mirror, there is a broad plateau extending up to $k_t\simeq2k_L$ due to the sharp decay of the atomic density as well as to its additional periodicity inside the mirror (see Fig. 4 and in particular the inset of the second panel).

The atomic standing waves considered in this section correspond to a one-dimensional lattice with a uniform and possibly large filling factor. The number of mutually coherent lattice periods is only limited by the coherence length of the atom laser beam. Such atomic standing waves may lead to interesting applications in much the same way as done for x-ray standing waves [21].

ACKNOWLEDGMENT

It is a pleasure to thank Markus Greiner for fruitful discussions.

[1] M. H. Anderson *et al.*, Science **269**, 198 (1995); K. B. Davis *et al.*, Phys. Rev. Lett. **75**, 3969 (1995); C. C. Bradley *et al.*, *ibid.* **75**, 1687 (1995).

[2] M. O. Mewes *et al.*, Phys. Rev. Lett. **78**, 582 (1997); I. Bloch *et al.*, *ibid.* **82**, 3008 (1999); E. W. Hagley *et al.*, Science **283**, 1706 (1999).

[3] H. M. Wiseman, Phys. Rev. A **56**, 2068 (1997); Y. Japha *et al.*, Phys. Rev. Lett. **82**, 1079 (1999); M. Naraschewski and R. J. Glauber, Phys. Rev. A **59**, 4595 (1999).
[4] J. Stenger *et al.*, Phys. Rev. Lett. **82**, 4569 (1999); E. W. Hagley *et al.*, *ibid.* **83**, 3112 (1999); I. Bloch *et al.*, Nature (London) **403**, 166 (2000).
[5] B. W. Batterman and H. Cole, Rev. Mod. Phys. **36**, 681 (1964).
[6] J. M. Cowley, *Diffraction Physics* (North-Holland, Amsterdam, 1981).
[7] See, e.g., *Confined Electrons and Photons*, edited by E. Burstein and C. Weisbuch (Plenum Press, New York, 1995).
[8] M. K. Oberthaler *et al.*, Phys. Rev. A **60**, 456 (1999).
[9] N. Friedman *et al.*, J. Opt. Soc. Am. B **15**, 1749 (1998).
[10] M. Weidemüller *et al.*, Phys. Rev. Lett. **75**, 4583 (1995).
[11] C. Cohen-Tannoudji, J. Dupont-Roc, and G. Grynberg, *Processus d'Interaction entre Photons et Atomes* (InterEditions/ Editions du CNRS, Paris, 1988).
[12] G. Bassani and G. Pastori Parravicini, *Electronic States and Optical Transitions in Solids* (Pergamon Press, Oxford, 1975); P. Y. Yu and M. Cardona, *Fundamentals of Semiconductors* (Springer, Berlin, 1996).
[13] M. Wilkens *et al.*, Phys. Rev. A **44**, 3130 (1991).
[14] See, e.g., M. J. Renn *et al.*, Phys. Rev. Lett. **75**, 3253 (1995); D. Müller *et al.*, *ibid.* **83**, 5194 (1999).
[15] I. Carusotto and G. C. La Rocca, Phys. Rev. Lett. **84**, 399 (2000); in *Proceedings of the XXVII International School of Quantum Electronics, Erice, 1999*, edited by S. Martellucci, A. Chester, M. Inguscio, and A. Aspect (Kluwer Academic/ Plenum Publishers, London, 2000).
[16] P. N. Butcher and D. Cotter, *The Elements of Nonlinear Optics* (Cambridge University Press, Cambridge, 1993).
[17] R. Loudon, *The Quantum Theory of Light* (Clarendon Press, Oxford, 1973); D. F. Walls and G. J. Milburn, *Quantum Optics* (Springer-Verlag, Berlin, 1994).
[18] C. W. Gardiner, *Handbook of Stochastic Methods* (Springer-Verlag, Berlin, 1985).
[19] We are indebted to Markus Greiner for an illuminating discussion on this point.
[20] O. Morice *et al.*, Phys. Rev. A **51**, 3896 (1995); M. R. Andrews *et al.*, Science **273**, 84 (1996).
[21] J. Zegenhagen, Surf. Sci. Rep. **18**, 1 (1993).